

# Rovibrational state mixing in the aldehyde C–H stretch fundamental region of acetaldehyde

H. L. Kim,<sup>a)</sup> T. K. Minton,<sup>b)</sup> R. S. Ruoff, T. J. Kulp,<sup>c)</sup> and J. D. McDonald  
*School of Chemical Sciences, University of Illinois, Urbana, Illinois 61801*

(Received 16 May 1988; accepted 15 June 1988)

We have studied rovibrational state mixing in acetaldehyde using infrared laser induced fluorescence. Molecules are isolated and cooled in supersonic molecular beams, and irradiated in the C–H stretch fundamental region with an infrared optical parametric oscillator. Spectral resolution is provided with either a circular variable filter machine or a cryogenic Michelson interferometer. We have found evidence of several strong Fermi resonances between the aldehyde C–H stretch and a few overtones and combinations of lower frequency modes. In addition, there is substantial random state mixing in this region as evidenced by the average experimental dilution factor of 0.2. The dependence of the dilution factor on the average  $J$  excited by the laser shows that the extent of state mixing scales linearly with  $J$ . We have observed from dispersed fluorescence spectra that random rotational coupling occurs between different  $K_p$  states. Our previous statistical coupling model has been applied to the interpretation of the data, and its applicability is discussed. For the model calculation, the methyl torsion is specially treated as a very anharmonic mode in the enumeration of the zeroth order bath states. The average coupling width derived from the model calculation is  $0.35 \text{ cm}^{-1}$ . The relative energy content apportioned among vibrational modes in the molecule following excitation is measured and is successfully explained with the model.

## I. INTRODUCTION

Previous work in our laboratory has characterized intramolecular vibrational energy redistribution (IVR) in terms of mixing of zeroth order basis states by studying infrared fluorescence from the C–H stretch fundamental region of a variety of molecules following excitation with a medium resolution ( $1\text{--}2 \text{ cm}^{-1}$  bandwidth) laser.<sup>1–4</sup> The extent of state mixing has been derived from the measurement of the dilution factor, which is inversely related to the average number of molecular eigenstates that couple to a single zeroth order optically active state. Earlier experiments in our group showed clearly that rotational–vibrational (i.e., Coriolis) interactions were important in state mixing,<sup>5,6</sup> and the recent detailed study on norbornadiene<sup>7</sup> has advanced our understanding of the effect of these rovibrational interactions with the application of a statistical coupling model. This model assumes that the “zeroth order optically active state,” discussed by many authors, is a rovibrational state, as opposed to just a vibrational state. The optically inactive “bath states” are, therefore, also taken to be rovibrational states. The model successfully explained the extent of state mixing (represented by the experimental dilution factors), the observed linear  $J$  dependence of state mixing, and the relative energy contents in the vibrational modes that are mixed with the initially excited state.

Although the model describes well state mixing in the large asymmetric molecule, norbornadiene, its applicability

to smaller and/or more symmetric species (which show evidence of state mixing) remains uncertain. For example, the model assumes only the minimum requirements for coupling—conservation of total angular momentum  $J$  and of overall symmetry, but in a symmetric or near symmetric top molecule, coupling could have an additional  $K$  quantum number dependence. In small near symmetric tops,<sup>8,9</sup> coupling strength has been found to depend on  $J$  and  $K$  quantum numbers through first order Coriolis interactions. Furthermore, small molecules might exhibit specific, albeit random, couplings as seen in propynal.<sup>6</sup> For the model to be able to predict such specific, random coupling in a molecule, its spectroscopy would have to be known in great detail, which is usually not the case. And more importantly, the model would lose its usefulness as a simple description of state mixing in the limit of a molecule small enough to be handled by conventional spectroscopy. Propynal probably represents this limit.

We chose, therefore, to perform an IR fluorescence study of state mixing in the C–H stretch fundamental region of acetaldehyde, the smallest molecule in which we have seen evidence of extensive state mixing. In addition to its small size, it is a near prolate top; thus, the  $B$ -type rotational band contour of the aldehyde C–H stretch has resolvable  $Q$ -branch subbands for different transitions in the  $K_{\text{prolate}}$  quantum number. Excitation of various subbands would be a good way to probe any possible  $K$  dependence on state mixing. Because of its size and symmetry, acetaldehyde is a prime candidate for a study of specific couplings and coupling constraints, which would suggest modifications to our present statistical model.

As will be seen, all the data on acetaldehyde can be explained by combining the present model, which only had to be modified slightly in order to treat the methyl torsional

<sup>a)</sup> Present address: Department of Chemistry, Columbia University, New York, New York 10027.

<sup>b)</sup> Present address: Physikalisch-Chemisches Institut der Universität, Winterthurerstr. 190, CH-8057 Zürich, Switzerland.

<sup>c)</sup> Present address: Lawrence Livermore National Laboratory, Livermore, California 94550.

mode as a very anharmonic mode, with the conventional picture of Fermi resonance—i.e., we see *several* strong Fermi resonance couplings of the C–H stretch to very simple overtones and combinations in addition to random coupling to more complex nearby states. The extent of state mixing is observed to scale linearly with  $J$ —the same result that was found in the norbornadiene experiment.

## II. EXPERIMENT

The experimental apparatus and procedures are described in detail in previous papers<sup>1,2</sup> except for the case of high resolution interferometer scans. Acetaldehyde, obtained from Aldrich, is purified by trap-to-trap distillation. The vapor of the liquid chemical at 15 °C is seeded in air at ambient pressure and supersonically expanded into a vacuum through a pulsed nozzle. With this beam condition, no evidence has been found of signal due to van der Waals clusters, and the rotational temperature in the beam was determined to be 45 K. Molecules are irradiated in the C–H stretch region of the spectrum by an infrared optical parametric oscillator, and fluorescence spectra are measured with either a circular variable filter machine or a Michelson interferometer (Digilab model 296 interferometer with modification for liquid nitrogen temperature operation). Normal operation of the interferometer with a 1024 point interferogram gives about  $8\text{ cm}^{-1}$  resolution (Fig. 2). However, an increase in the number of data collection points (2048 point interferogram) by increasing the distance of the mirror movement increases the resolution by a factor of about 2 (Fig. 3). Einstein  $A$  coefficients for the vibrational bands of acetaldehyde were obtained from a gas phase IR absorption spectrum taken with a Nicolet FT-IR spectrophotometer (Table I).

## III. RESULTS AND ANALYSIS

The main vibrational band studied in this experiment was the aldehyde C–H stretch fundamental ( $\nu_3$ ), centered at  $2708\text{ cm}^{-1}$ , and its Fermi resonance companions. The low resolution ( $1\text{--}2\text{ cm}^{-1}$ ) fluorescence excitation spectrum of this band is shown in Fig. 1. This spectrum consists of many

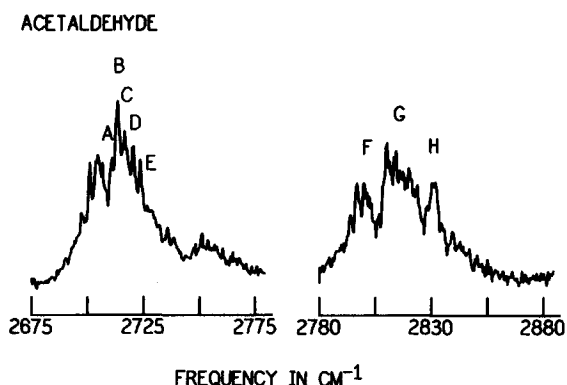


FIG. 1. Fluorescence excitation spectra of the bands of acetaldehyde studied. Labels indicate the different laser excitation positions where dispersed fluorescence spectra were measured.

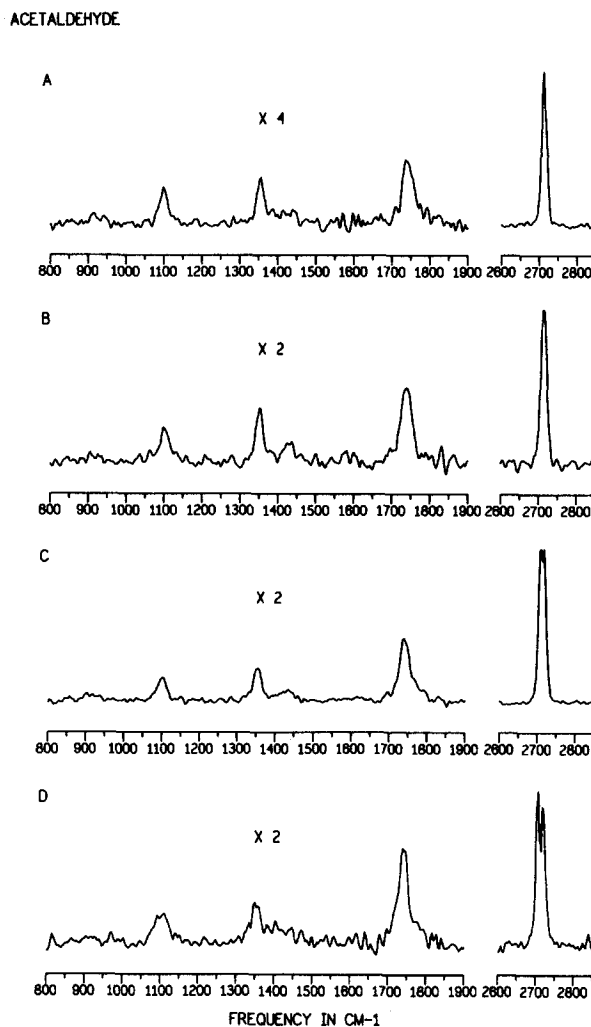


FIG. 2. Dispersed fluorescence spectra of acetaldehyde obtained from the laser excitation positions indicated in Fig. 1.

partially resolved peaks which are  $Q$ -branch subbands, each one corresponding to a particular  $\Delta K_p$  rotational transition. Such a spectrum is typical for a  $B$ -type contour band of a near prolate top molecule.<sup>10</sup> In addition, combination and overtone bands are seen around  $2800\text{ cm}^{-1}$  in the spectrum. Hollenstein and Günthard<sup>11</sup> have found two  $B$ -type bands at  $2807$  and  $2830\text{ cm}^{-1}$ , although they are not clearly resolved. They assigned the  $2830\text{ cm}^{-1}$  band as the first overtone of the in-plane C–H wag ( $\nu_6$  at  $1395\text{ cm}^{-1}$ ) while the other band at  $2807\text{ cm}^{-1}$  remained unassigned. However, according to our own absorption and dispersed fluorescence spectra from these bands (which will be discussed in detail later in this section), we have assigned the band at  $2830\text{ cm}^{-1}$ , instead of  $2\nu_6$ , as the combination of  $\nu_6$  with the asymmetric  $\text{CH}_3$  deformation ( $\nu_5$  at  $1434\text{ cm}^{-1}$ ), and the other band at  $2808\text{ cm}^{-1}$  as either the  $2\nu_6$  or the combination of  $\nu_5$  and  $\nu_7$  (symmetric  $\text{CH}_3$  deformation at  $1352\text{ cm}^{-1}$ ). Evidence of Fermi resonance has also been found between these bands and the  $\nu_3$  band at  $2708\text{ cm}^{-1}$ . We have performed a band contour simulation using the known rotational constants<sup>13</sup> ( $A, B, C = 1.888, 0.339, 0.334\text{ cm}^{-1}$ ), and we have thus derived a rotational temperature of 45 K for our experimen-

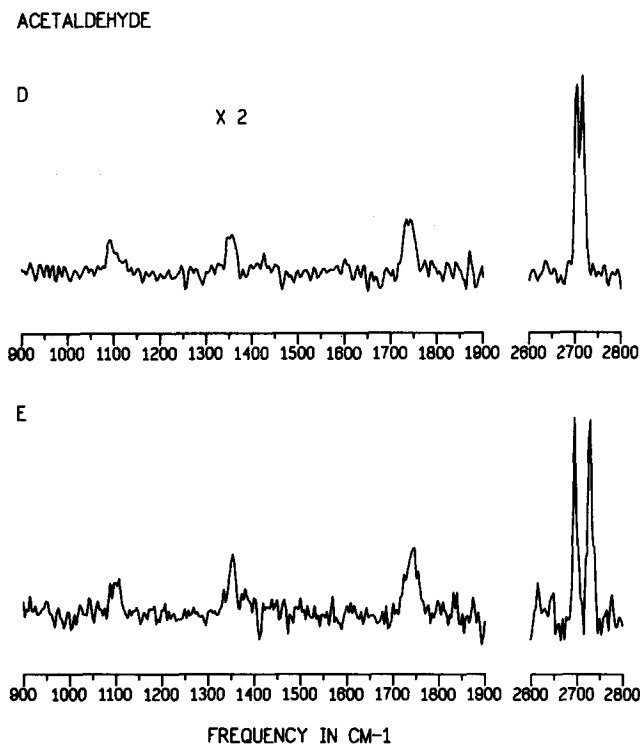


FIG. 3. Dispersed fluorescence spectra of acetaldehyde obtained from the laser excitation positions, D and E, in Fig. 1 with high resolution ( $\sim 5$   $\text{cm}^{-1}$ ).

tal fluorescence excitation spectrum of the  $2708\text{ cm}^{-1}$  band.

The average dilution factor for the  $\nu_3$  band was measured using the procedure described in previous papers. The resonance fluorescence excitation spectrum is required for this measurement, and while it is not shown, its appearance is similar to the total fluorescence excitation spectrum shown in Fig. 1. Since the bands in the  $2800\text{ cm}^{-1}$  region are combinations and overtones, no attempt has been made to measure the dilution factor for these bands. As a calibration standard for the dilution factor determination, three well studied C-H stretch bands ( $\nu_0 = 2947, 2980,$  and  $2998\text{ cm}^{-1}$ ) of norbornadiene were used.<sup>7</sup> The measured dilution factor is 0.2, which suggests substantial state mixing for such a small molecule.

Dispersed fluorescence spectra have been collected for the different laser excitation positions shown in Fig. 1, and they are presented in Figs. 2, 3, and 4. The spectra in Fig. 3

TABLE I. Measured Einstein  $A$  coefficients for the vibrational bands of acetaldehyde.

Band position ( $\text{cm}^{-1}$ )	$A_0^1$ ( $\text{s}^{-1}$ )
2830	29.14
2715	16.54
1745	8.85
1434	0.77
1395	0.73
1352	0.42
1114	0.82
867	0.09

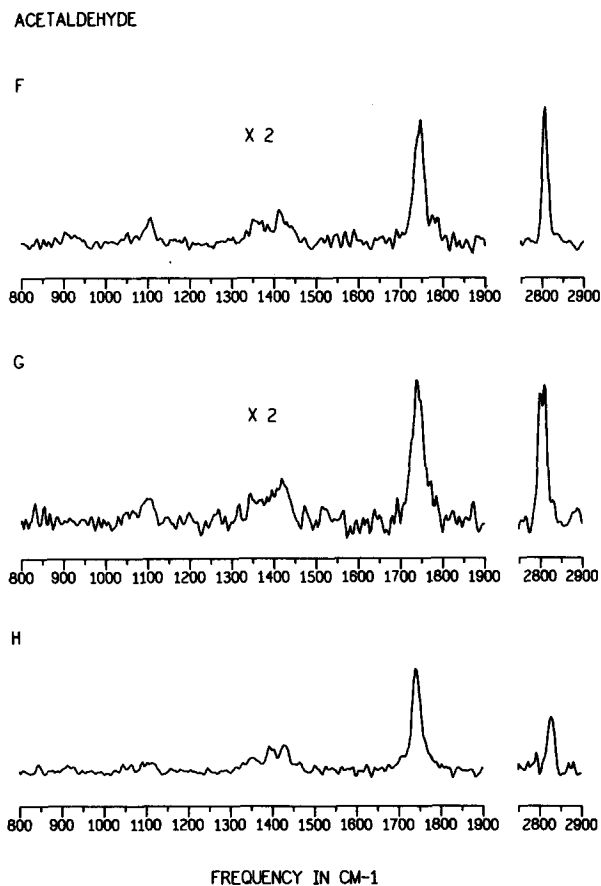


FIG. 4. Dispersed fluorescence spectra of acetaldehyde from the laser excitation positions, F, G, and H, in Fig. 1.

are of higher resolution ( $\sim 5\text{ cm}^{-1}$ ) than those in Figs. 2 and 4 ( $\sim 8\text{ cm}^{-1}$ ). In the nonresonance fluorescence region, three major peaks can be seen at  $1743, 1358,$  and  $1114\text{ cm}^{-1}$ . In addition, broad features are visible around  $1400\text{ cm}^{-1}$ . The peaks at  $1743$  and  $1114\text{ cm}^{-1}$  are easily assigned as the C=O stretch ( $\nu_4$ ) and the C-C stretch ( $\nu_8$ ) fundamentals, respectively. Between  $1300$  and  $1450\text{ cm}^{-1}$ , three fundamentals have been assigned as the symmetric and asymmetric  $\text{CH}_3$  deformation at  $1352\text{ cm}^{-1}$  ( $\nu_7$ ) and  $1433\text{ cm}^{-1}$  ( $\nu_5$ ), respectively, and the in-plane C-H wag at  $1395\text{ cm}^{-1}$  ( $\nu_6$ ). The band at  $1358\text{ cm}^{-1}$  in Figs. 2 and 3 shows exceptionally strong fluorescence compared to the other bands. In addition, the fact that there is no fundamental assigned at  $1358\text{ cm}^{-1}$  suggests a possible Fermi resonance between  $\nu_3$  and the other bands seen in the C-H stretch region. However, the strong fluorescence at  $1358\text{ cm}^{-1}$ , which results from excitation of the  $\nu_3$  band, cannot be ascribed to a Fermi resonance with any bands actually visible in the  $2800\text{ cm}^{-1}$  region shown in Fig. 1. Instead, this band must arise from a weak Fermi resonance involving  $2\nu_7$  (at  $2704\text{ cm}^{-1}$ ) and  $\nu_3$ , which is not seen in the spectrum in Fig. 1 because of the wide and strong  $\nu_3$  band. As a result of Fermi resonance, its frequency is shifted upward by about  $6\text{ cm}^{-1}$  from the fundamental frequency of  $\nu_7$  (at  $1352\text{ cm}^{-1}$ ). We have thus assigned the  $1358\text{ cm}^{-1}$  band as the Fermi resonance fluorescence from the  $\nu_7$  component of the  $\nu_3$  band. We have as-

signed the band at  $2830\text{ cm}^{-1}$  in Fig. 1 as  $\nu_5 + \nu_6$ . This assignment is based on the dispersed fluorescence spectrum labeled as H in Fig. 4. The spectrum shows weak resonance fluorescence and strong nonresonance fluorescence at the fundamental frequencies of  $\nu_5$  and  $\nu_6$  at  $1395$  and  $1434\text{ cm}^{-1}$ , respectively, in addition to the fluorescence from extensive state mixing in this region. Fluorescence spectra from the  $2808\text{ cm}^{-1}$  band (F for low  $J$  and  $K_p$  excitation and G for higher  $J$  and  $K_p$  excitation) also show evidence of Fermi resonance. If we assign this band as  $2\nu_6$  (with a frequency shift upward by about  $20\text{ cm}^{-1}$ ) in Fermi resonance with the  $\nu_3$  band, the fluorescence frequency of the  $\nu_6$  band should also be shifted upward by  $20\text{ cm}^{-1}$ , resulting in the observed fluorescence at  $1415\text{ cm}^{-1}$ . On the other hand, excitation of the  $\nu_3$  band should result in a downward frequency shift of the  $\nu_6$  "unrelaxed" fluorescence from its fundamental frequency.

As the laser excitation position is moved farther away from the band center, higher  $K_p$  states can be excited. With our interferometer resolution, two peaks have been clearly resolved in the resonance fluorescence region when the pump position is at E (average  $K_p$  excited is about 5). According to the selection rules for a type B transition in a near prolate top, these two peaks arise from  $\Delta K_p = \pm 1$  rotational transitions. Separation of these two transitions can be approximately calculated with known rotational constants and average  $K_p$  values derived from the contour simulation. The calculated separation is found to be  $32\text{ cm}^{-1}$  when the pump is at E, which is in good agreement with the  $34\text{ cm}^{-1}$  separation measured from the spectrum in Fig. 3.

Dilution factors for each laser excitation position of the  $\nu_3$  band have been measured from the dispersed fluorescence spectra. Since the peaks at  $1743$  and  $1114\text{ cm}^{-1}$  are well separated from the other peaks, experimental dilution factors are measured from these two peaks. The dilution factors derived from the dispersed fluorescence spectra have slightly lower values than those from the resonance fluorescence spectra. This discrepancy has been discussed in the previous paper.<sup>7</sup> One cause is the fact that the calculation of dilution factors from the dispersed fluorescence spectra assumes that the character of the zeroth order optically active state  $|s\rangle$  is spread equally among a set of bath states. This assumption might not hold true in a small molecule such as acetaldehyde. On the other hand, the derivation of the dilution factor from the resonance fluorescence excitation spectra does not involve any assumptions, although the experimental errors are relatively large. Furthermore, the two dilution factors are not even in principle the same. The dispersed fluorescence measurement should give the average dilution factor in the fairly small energy width excited by the laser, while the resonance fluorescence measurement is the average  $\phi_d$  for the whole vibrational band.

Measured dilution factors are listed in Table II. In order to find a functional dependence of the dilution factors in terms of the band position, average rotational quantum numbers of the states excited with the laser for each band position have been found from the contour simulation. Normalized reciprocal rotational quantum numbers are plotted as a function of the band position in Fig. 5 together with the

TABLE II. Measured and calculated dilution factors for various excitations of acetaldehyde.

Band position ( $\text{cm}^{-1}$ )	$\langle\phi_d\rangle_{\text{exp}}^a$	$\langle\phi_d\rangle_{\text{calc}}^b$
2708 <sup>c</sup>	0.197	0.191
2710	$0.059 \pm 0.018$	$0.195 \pm 0.103$
2712	$0.033 \pm 0.010$	$0.222 \pm 0.121$
2716	$0.049 \pm 0.015$	$0.203 \pm 0.102$
2719	$0.034 \pm 0.010$	$0.202 \pm 0.106$
2728	$0.029 \pm 0.012$	$0.188 \pm 0.109$

<sup>a</sup> Obtained from  $1114$  and  $1743\text{ cm}^{-1}$  bands in dispersed fluorescence spectra. Calculated errors are  $\pm 1\sigma$  derived from the noise in the spectra and estimated from errors in  $A$  coefficient measurements.

<sup>b</sup> Obtained from the model calculation with the coupling width of  $0.35\text{ cm}^{-1}$ .

<sup>c</sup> Dilution factors for the whole vibrational band obtained from the resonance fluorescence spectrum and the model calculation. Estimated experimental error is about 50%.

dilution factors. Several attempts have been made to find a functional dependence for the inverse of the dilution factors (the number of coupled states). The measured dilution factors are found to be close to the function of  $\langle J \rangle^{-1}$ .

Relative energy contents of the modes whose frequencies are observed in our dispersed fluorescence spectra are measured from the relative areas of the peaks. The measured relative energy contents for the  $1358\text{ cm}^{-1}$  band appear anomalously high compared to the others as a result of the Fermi resonance. In addition, since the  $1358\text{ cm}^{-1}$  band (shifted from its fundamental frequency of  $1352\text{ cm}^{-1}$ ) is badly overlapped with the fundamental at  $1395\text{ cm}^{-1}$ , these bands are ignored in the relative energy content plot in Fig. 6. As can be seen, the energy content is higher for lower frequency fundamentals because a lower frequency mode can be involved in more combinations and overtones in a given energy region than can a higher frequency mode.

As mentioned in the Introduction, we have employed a statistical state mixing model in order to test its predictive capabilities for a small molecule such as acetaldehyde. The model is used to predict dilution factors, the  $J$  dependence of the dilution factors, and the relative energy contents of the vibrational modes that participate in the makeup of the molecular eigenstates that are excited with the laser. The only adjustable parameter is the average energy width over which the character of a zeroth order optically active state is spread. This average coupling width can thus be derived if the model renders a reasonably good picture of state mixing in the molecule.

The model has been described in detail before,<sup>7</sup> so we will only outline its key elements here. The basic assumption of the model is that every rovibrational state (in a particular vibrational band) that can be excited by a laser of a given bandwidth is to be treated as a zeroth order optically active state  $|s_i\rangle$ . Therefore, each of these states can mix with optically inactive zeroth order rovibrational bath states  $\{|l_j\rangle\}$  to form a "clump" of molecular eigenstates. For each  $|s_i\rangle$  state, a dilution factor is calculated, which is taken to be

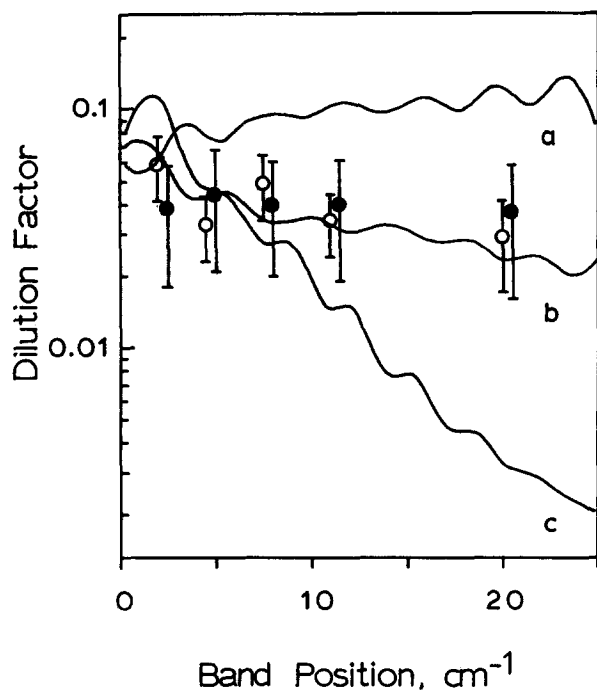


FIG. 5. Dilution factors and rotational quantum numbers as a function of band position of the  $\nu_3$  band of acetaldehyde. Open circles represent the dilution factors measured from dispersed fluorescence spectra, and closed circles are those from our model calculation. Curves, a, b, and c show the functional dependence upon the average rotational quantum numbers:  $|J - K_p|^{-1}$ ,  $J^{-1}$ , and  $K_p^{-1}$ , respectively. All the curves are normalized to the experimental dilution factors.

$(N + 1)^{-1}$ , where  $N$  is the number of bath states that couple to the given  $|s_i\rangle$  state. (Note that implicit in this calculated dilution factor is the assumption that all bath states couple equally to  $|s_i\rangle$ .) The assumed constraints on coupling are only conservation of overall rovibrational symmetry and total angular momentum  $J$ . The adjustable coupling width is, of course, also a constraint. Because many  $|s\rangle$  states can be excited simultaneously by our medium resolution laser, we take a weighted average of the dilution factors corresponding to each  $|s_i\rangle$  state in order to obtain the final "experimental" dilution factor. The weighting factors are the transition probabilities to each final  $|s_i\rangle$  state. The relative energies in all the vibrational modes that are excited as a result of state mixing are found by first summing the number of quanta in each mode that makes up a given  $|j\rangle$  state over the  $N$  bath states that mix with each final  $|s_i\rangle$  state. The average (relative) mode content is then calculated by taking the weighted average of mode contents corresponding to each  $|s_i\rangle$  state, where the weighting factors are again the transition probabilities to the final  $|s\rangle$  states. The relative energy contents follow directly from the relative mode contents. The whole calculation is repeated for many center energies of the laser in order to average out the effects of using the rigid rotor-harmonic oscillator approximation, which is used to calculate all the zeroth order states. Such effects could be manifested in the prediction of artificially strong or weak mixing resulting from an accidental pile up or sparsity of calculated bath states in a particular energy region.

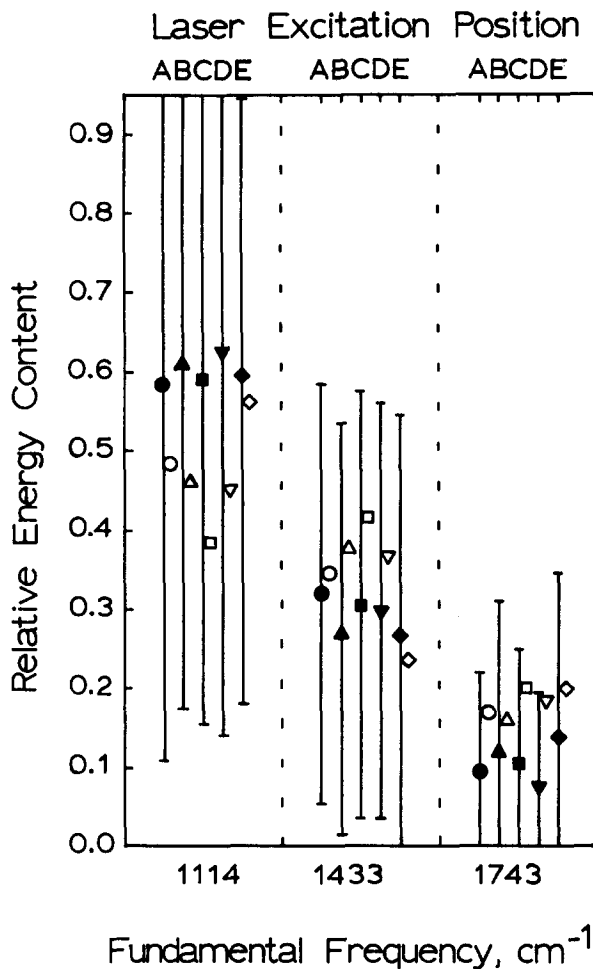


FIG. 6. Plot of the relative energy contents of vibrational modes seen in dispersed fluorescence spectra of acetaldehyde, normalized such that the sum of the energy content of the modes for each laser excitation position is one. Open symbols represent experimental energy contents, and closed symbols are those from the model calculation. Uncertainties for the experimental energy contents are much smaller than the error bars on the calculated points.

While the model as previously applied to norbornadiene assumed every mode to be harmonic, the methyl group torsional mode in acetaldehyde must be specially treated because of its anharmonicity, which greatly enhances the number of bath states. In order to assign the symmetry of torsional energy levels, molecular symmetry group theory has been applied. According to Bunker,<sup>12</sup> acetaldehyde is in the  $C_{3v}(M)$  symmetry group, and has  $A_1$ ,  $A_2$ , and  $E$  irreducible representations. Using the  $\cos 3\phi$  potential for a hindered rotor with the known barrier height<sup>13</sup> of  $406 \text{ cm}^{-1}$ , torsional energy levels have been calculated with proper symmetry assignments. Assuming the other vibrational modes to be harmonic (Table III), all the zeroth order bath states are calculated as combinations and overtones including rotational states. Since the first excited torsional levels ( $E$  symmetry) are so close (less than  $1 \text{ cm}^{-1}$ ) to the ground state ( $A_1$  symmetry), these levels are thermally populated prior to the laser excitation. As a result, the laser can excite combinations of both symmetries in the C-H stretch region. Thus,

TABLE III. Fundamental frequencies and symmetries of vibrational modes of acetaldehyde used in model calculation,  $\text{cm}^{-1}$ .

Symmetry of torsional energy levels	
$ m ^a$	$\Gamma_{\text{tot}}$
0	$A_1$
$3n \pm 1$	$E$
$3n$	$A_1$ or $A_2$

<sup>a</sup>  $n$  is integral.

the dilution factors and energy contents of the modes are calculated for the states of both  $E$  and  $A_1$  symmetries, and weighted averages are taken. The weighting factors are statistically obtained assuming equal populations of the ground and each of the first excited torsional levels. The calculated dilution factor for the whole  $\nu_3$  band is close to the experimental one (0.2) when we assumed the average coupling width to be about  $0.35 \text{ cm}^{-1}$ .

Dilution factors for each laser excitation position of the  $\nu_3$  band shown in Fig. 1 are calculated with the average coupling width of  $0.35 \text{ cm}^{-1}$ . Calculated dilution factors are listed in Table II and plotted against band positions in Fig. 5. They are slightly higher than the measured dilution factors. However, considering the simplicity of the model, they are in reasonably good agreement, as can be seen in the figure.

Our proposed state mixing model also explains the relative energy apportioned among vibrational modes in the molecule. The relative energy contents of the modes whose fluorescence is seen in the dispersed fluorescence spectra are calculated from the model. Since the calculated energy contents strongly depend upon the exact frequencies of the bath states, they are averaged over the whole region of the C–H stretch fundamental. Measured and calculated relative energy contents of modes at 1114, 1433, and 1743  $\text{cm}^{-1}$  are presented in Fig. 6. Each calculated energy content represents the average of 51 calculations ( $\pm 25 \text{ cm}^{-1}$  from the laser excitation position), and each error bar is  $\pm 1\sigma$  of this average value. As can be seen in the figure, our state mixing model can qualitatively predict the relative energy contents of the modes, although the enormous error bars suggest the large variation in the bath state mode contents, as can be expected at low state densities.

#### IV. DISCUSSION

Acetaldehyde, with its seven atoms, is a fairly small molecule. However, its structure which includes a methyl rotor leads to substantial state mixing in the C–H stretch fundamental region. The density of rovibrational bath states adjusted for the correct  $J$  and symmetry to couple locates this molecule at the lower edge of the transition region for the onset of state mixing as seen in the curve empirically obtained by Kim *et al.*<sup>6</sup> With the vibrational modes treated as harmonic except for the methyl torsion, the calculated rovibrational state density of  $E$  symmetry in the C–H stretch region is about 55 states per  $\text{cm}^{-1}$ , while the state density for  $A_1$  or  $A_2$  symmetry is about 13 states per  $\text{cm}^{-1}$ . Since the

direct product of  $E$  with  $A_1$  or  $A_2$  symmetry is  $E$ , states of  $E$  symmetry are dominant in the bath states, because most of the bath states involve combinations and overtones of torsional states with  $E$  symmetry. Therefore, the presence of the methyl rotor increases the state density enough for state mixing to occur. In several spectroscopic studies, the “floppiness” of the molecule has been found to influence the extent of state mixing. A certain low frequency mode has been found in some aromatic molecules<sup>14–16</sup> in the  $S_1$  excited electronic state which enhances the extent of state mixing although no single mechanism has been identified. Parmenter and co-workers<sup>17</sup> have suggested that in *p*-fluorotoluene, the methyl torsion can increase state mixing via van der Waals interaction with the benzene ring. However, when the methyl group torsional mode is specially treated as a very anharmonic mode, a simple analysis of the state density and of the symmetry of the states available for coupling can, within the context of our coupling model, explain state mixing in acetaldehyde.

The coupling width over which the optical character of initially excited state is spread has been indirectly found from our model to be about  $0.35 \text{ cm}^{-1}$ . Compared to the values found in other studies, for example,  $0.05 \text{ cm}^{-1}$  in norbornadiene<sup>7</sup> and in 1-butyne,<sup>18</sup> and on the order of  $0.1 \text{ cm}^{-1}$  in methyl formate,<sup>19</sup> the coupling width of  $0.35 \text{ cm}^{-1}$  is slightly higher, which might show a difference in the average coupling strength between the  $\nu_3$  mode and the bath states. In order to draw any conclusion, a more systematic structural study on coupling strength would be needed. Nevertheless, the presence of a methyl rotor which could possibly interact strongly with the C–H stretch might account for the larger coupling width.

In the previous experiment on norbornadiene, the extent of state mixing scales linearly with the average  $J$  excited, which justifies the assumption of random rotational couplings between the states of different  $K$  quantum numbers. One might argue that since norbornadiene is a very asymmetric top molecule, rotational  $K$  quantum numbers may not be good quantum numbers and hence the selection rule for the coupling may be broken down. In small prolate top molecules, the extent of vibrational state coupling via a Coriolis mechanism has been found to be proportional to first order Coriolis matrix elements such as  $|J - K_p|$  or  $K_p$ . However, as can be seen in Fig. 5, measured and calculated dilution factors do not depend on  $K_p$ , rather, they follow closely  $\langle J \rangle^{-1}$ . Even in acetaldehyde which is a small near symmetric top molecule, no evidence of rotationally specific coupling has been found. The extent of state mixing is linearly proportional to the average  $J$  excited, which is to be expected since the number of bath states available for coupling increases as  $2J + 1$ .

Furthermore, this random rotational state mixing is manifested in our dispersed fluorescence spectra. In our own FT-IR absorption spectra and in the assignments by Hollenstein and Günthard,<sup>11</sup> the band at  $1114 \text{ cm}^{-1}$  has the same  $B$ -type band contour as the C–H stretch fundamental. Consequently, if there is no coupling between different  $K_p$  states, the  $1114 \text{ cm}^{-1}$  band should show the same splitting as the resonance fluorescence. However, the band at  $1114 \text{ cm}^{-1}$

shows an unresolved splitting as a result of more  $\Delta K_p$  rotational transitions than exhibited by the resonance fluorescence band (Fig. 3). This unresolved splitting is a clear evidence of at least some random rotational mixing of different  $K_p$  states. If the resolution of the laser were high enough to excite a single  $K_p$  state and if the resolution of the interferometer were also high, then the actual coupling between the different  $K_p$  states could be monitored.

Acetaldehyde shows complicated Fermi resonances between vibrational states in the C–H stretch region, which would make the application of our statistical state mixing model rather difficult. However, as shown in Fig. 6, our model explains reasonably well the relative energy apportioned among the bath modes, excluding those states involved in very low-order Fermi resonances. The error bars do not represent the uncertainty in the calculation. Instead, they reveal the nature of the bath states in the region studied. In a low state density molecule like acetaldehyde, the error bars are expected to be large simply because of wild fluctuations of the bath state mode contents. As the bath state density becomes higher, the error bars would be smaller.

#### ACKNOWLEDGMENT

This work was supported by the National Science Foundation under Grant No. NSF CHE87-17046.

<sup>1</sup>G. M. Stewart and J. D. McDonald, *J. Chem. Phys.* **78**, 3907 (1983).

<sup>2</sup>G. M. Stewart, M. D. Ensminger, T. J. Kulp, R. S. Ruoff, and J. D. McDonald, *J. Chem. Phys.* **79**, 3190 (1983).

<sup>3</sup>G. M. Stewart, R. Ruoff, T. Kulp, and J. D. McDonald, *J. Chem. Phys.* **80**, 5353 (1984).

<sup>4</sup>T. Kulp, R. Ruoff, G. M. Stewart, and J. D. McDonald, *J. Chem. Phys.* **80**, 5359 (1984).

<sup>5</sup>T. J. Kulp, H. L. Kim, and J. D. McDonald, *J. Chem. Phys.* **85**, 211 (1986).

<sup>6</sup>H. L. Kim, T. J. Kulp, and J. D. McDonald, *J. Chem. Phys.* **87**, 4376 (1987).

<sup>7</sup>T. K. Minton, H. L. Kim, and J. D. McDonald, *J. Chem. Phys.* **88**, 1539 (1988).

<sup>8</sup>B. E. Forch, K. T. Chen, H. Salgusa, and E. C. Lim, *J. Phys. Chem.* **87**, 2280 (1983).

<sup>9</sup>H. L. Dai, C. L. Korpa, J. L. Kinsey, and R. W. Field, *J. Chem. Phys.* **82**, 1688 (1985).

<sup>10</sup>G. Herzberg, *Molecular Spectra and Molecular Structure, Vol. 2, Infrared and Raman Spectra of Polyatomic Molecules* (Van Nostrand Reinhold, New York, 1945).

<sup>11</sup>H. Hollenstein and Hs. H. Günthard, *Spectrochim. Acta Part A* **27**, 2027 (1971).

<sup>12</sup>P. R. Bunker, *Vibrational Spectra and Structure*, edited by J. R. Durig (Dekker, New York, 1975).

<sup>13</sup>R. W. Kilb, C. C. Lin, and E. B. Wilson, Jr., *J. Chem. Phys.* **26**, 1695 (1957).

<sup>14</sup>S. H. Kable, W. D. Lawrance, and A. W. E. Knight, *J. Phys. Chem.* **86**, 1244 (1982).

<sup>15</sup>M. Fujii, T. Ebata, N. Mikami, M. Ito, S. H. Kable, W. D. Lawrance, T. B. Parsons, and A. W. E. Knight, *J. Phys. Chem.* **88**, 2937 (1984).

<sup>16</sup>D. L. Catlett, Jr., K. W. Holtzclaw, D. Krajnovitch, D. B. Moss, C. S. Parmenter, W. D. Lawrance, and A. W. E. Knight, *J. Phys. Chem.* **89**, 1577 (1985).

<sup>17</sup>D. B. Moss, C. S. Parmenter, and G. E. Ewing, *J. Chem. Phys.* **86**, 51 (1987).

<sup>18</sup>A. M. de Souza, D. Kaur, and D. S. Perry, *J. Chem. Phys.* **88**, 4569 (1988).

<sup>19</sup>Unpublished results in our laboratory from the measurement of the eigenstate spectra in the C–H stretch fundamental region of methyl formate with a high resolution OPO (0.003 cm<sup>-1</sup> bandwidth).